

Chapter 14

Modelling Potential Zones of Gangotri Glacier Using GIS and ML in the Wake of Physico-Climatic Factors



Zainab Khan, Mohd Mohsin, Uzma Ajmal, and Ateeque Ahmad

Introduction

Glaciers on Earth are important components of the climate system. Changes in glaciers are indicators of climate change (Forsberg et al., 2017), and they contribute to and sustain significant river systems on the face of the earth (Bolch et al., 2012; Verma et al., 2021). In total, 15–28% of run off is contributed by glaciers (Liljedahl et al., 2017), and thus their existence is viable for rivers and streams (Kong et al., 2019).

Himalayas are the largest adobe of ice and snow outside poles, and various mighty glaciers straddle in the Himalayan Valleys (Ramsankaran et al., 2021), covering an area of 33,000 km² (Bahuguna, 2003). These glaciers hold great ecological importance for the Indian sub-continent, as rivers draining the sub-continent acquire a considerable proportion of their recharge from them (Thayyen & Gergan, 2010; Jones et al., 2018). However, the past few decades have not been very favourable for glaciers due to climate change (Clark et al., 2002; Pörtner et al., 2022). It is claimed that colder areas are getting hot faster than the rest of the earth's average (Arndt and Schembri, 2015), rendering glaciers especially vulnerable. The Himalayan range recorded the second fastest warming on the earth after the poles, leaving glacial bodies highly susceptible to rapid meltdown (Banerjee & Shankar, 2013; Kargel et al., 2011). Several studies are strongly suggestive of glacier recession under rising temperatures in the Kumaun Himalayas (Bisht et al., 2018; Singh et al., 2018) and Garhwal Himalayas (Chaujar, 2009).

Z. Khan (✉) · U. Ajmal · A. Ahmad

Department of Geography, Faculty of Science, Aligarh Muslim University, Aligarh, India

M. Mohsin

Department of Civil engineering, Faculty of Engineering and Technology, Zakir Husain College of Engineering, Aligarh Muslim University, Aligarh, India

Gangotri is one such glacier resting in the Garhwal Himalayas with strong signs of retreat (Bhambri et al., 2012) and has been the focus of researchers due to its hydrological, fluvial and economic significance (Arora & Malhotra, 2023). Ambinakudige, 2010, applied optical remote sensing images to support the recession of Gangotri while Varugu & Rao, 2016, exploited the SAR dataset for assessing Gangotri. Shi et al. (2023) used dug deeper using sedimentary biological structure to delve into the ecology of these glaciers. The glacial variability in the context of space and time is also assessed (Joshi et al., 2020). In studies, sub-alpine tree extension was used to support the crunching Gangotri glacier over the past century. Most of these scholars attributed the declining glaciers to climate change. Scholars such as Mitra et al. (2009), Ambinakudige (2010), and Bhambri et al. (2012), also associate the retreat with warming temperatures; however, the role of physical characteristics of the catchment remained uncredited in the context of Gangotri glacier. Paxman et al. (2017) argue that underlying topography plays a key role in the dynamics of overlying ice mass in a mountain range. The influence of underlying physiography is believed to have an effect even on the ice sheets with gentler and uniform aspects and altitude (Gassen et al. 2015), and thus, zones of ablation and accumulation in a glacier are not the sole outcome of temperature, but other physiological characteristics (Yu et al., 2013). This sort of research work is limited to the context of Gangotri or Himalayan region for that matter. Singh et al. (2017) have attempted to associate glacial retreat with morphological zones; however, their impact on the glaciers was not studied. Local physiological construct of the glacier catchment is in situ factors. Climate change or global temperature rise are ex site factors influencing a glacier. Both in situ and ex situ factors and their complex interrelationship in association with climatic factors play a great part in glacial dynamics, and therefore, these causative factors must be considered in holistic glacial studies. Arguably, a catchment represents the fundamental unit of hydrological studies that is defined by underlying topography (Jarvis, 2012); therefore, it is rational to study glacial dynamics at the catchment level.

In this study, for the first time, an attempt is made to explain the complex interrelationships of physico-climatic factors using Random Forest Regression (RFR), their impact on Gangotri and tried to model the potential zone of ablation, equilibrium, and accumulation at catchment level. The aims to explain the impact of the topographic factors as well as the temperature on the glacial dynamics. The study also seeks to quantify the areal changes in the foresaid potential zones of the glacier by temporal comparison.

Study Area

Gangotri is an alpine glacier nestling in the central Himalayas, falling in the district of Uttarkashi, Uttarakhand (Fig. 14.1). Being one of the largest glacial deposits in the Himalayas (Naithani et al., 2001), Gangotri pertains massive hydrological and ecological significance. It is one of the major tributary glaciers of the river Ganges.

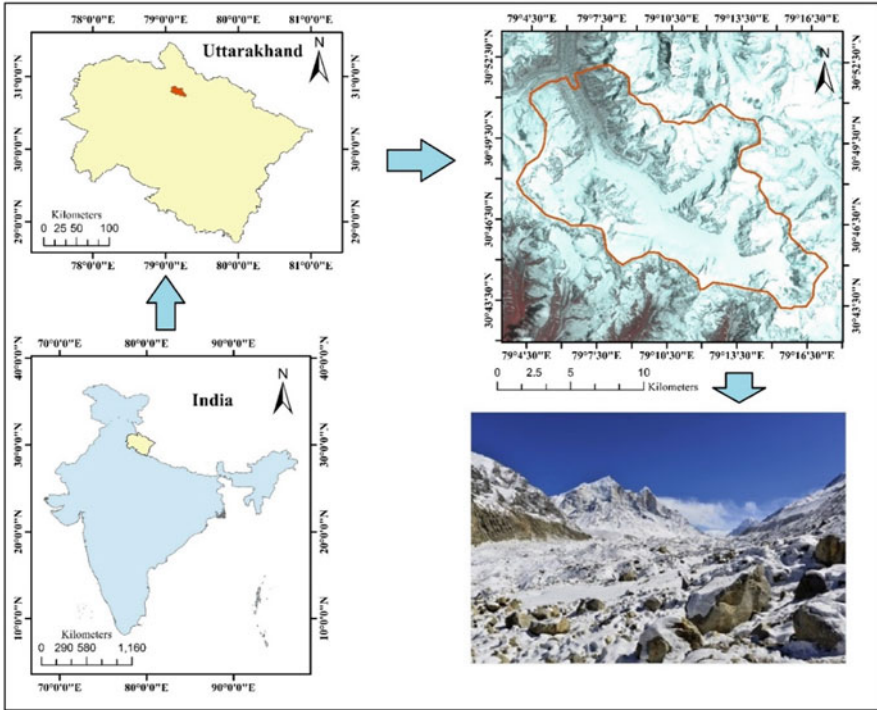


Fig. 14.1 Study area

Apart from that, Gangotri also has great mythological and religious importance in Hindu culture. The study area, i.e. catchment of Gangotri—the fundamental hydrological unit, is processed in a GIS environment. The processed glacial catchment covers 184 km^2 . There are massive variations in the altitude due to uneven topography. The altitude varies from 4474 m at its lowest point to 7085 m at its highest point across the catchment. The terrain of the catchment is full of undulation. This undulating terrain is also responsible for changing aspects over short distances causing uneven reception of the Sun's energy flux. Being curved by glacial ice, Gangotri sits in a U-shaped valley with a variant slope that ranges from 0° in the central part to 82° along the ridges. Hypsometric curve (Fig. 14.2) suggests that roughly 50% area of the catchment lies above 6500 m and roughly 95% area is above 5000 m ; therefore, it can be implied that almost all of the glacial catchment is above the snow-line (Ray, 2009).

A strong influence of aspect, slope and elevation can be visually observed in the maps. Aspect affects insolation and therefore determines temperature, slope determines movement under gravity and environmental lapse rate of temperature is controlled by elevation.

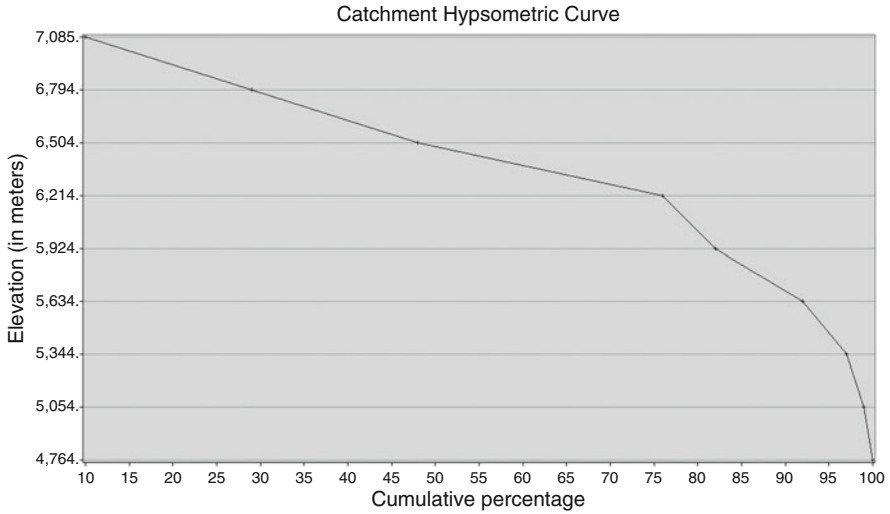


Fig. 14.2 Hypsometric curve of the catchment

Database and Methods

Database (Table 14.1)

Table 14.1 Data sources

| Satellite | Sensor | Bands used | Cloud cover | Source | Maps generated | Methods |
|-----------|--------------|------------------|-------------|---|----------------|--|
| Landsat 5 | TM | B2, B5, B6 | 0% | https://earthexplorer.usgs.gov/ | NDSI | NDSI (B2-B5/B2 + B5) |
| | | | | | LST | Mono window algorithm (band 6) |
| Landsat 8 | OLI and TIRS | B3, B6, B10, B11 | 0% | https://earthexplorer.usgs.gov/ | NDSI | NDSI (B3-B6/B3 + B6) |
| | | | | | LST | Split-window algorithm (bands 10 and 11) |
| Terra | ASTER | ASTER DEM | N.A. | https://earthexplorer.usgs.gov/ | Slope | Calculated in GIS environment |
| | | | | | Elevation | ASTER DEM |
| | | | | | Insolation | Estimated in GIS environment |

Rationale of Selection

Elevation

There is an inverse relationship between altitude, i.e. the mean height from sea level and temperature (Aigang et al., 2009); therefore, it seems fair to acknowledge altitude as one of the most important factors affecting the distribution of snow in a region. Altitude is the lone responsible factor for the accumulation of snow-clad regions in low latitudes in the form of alpine glaciers (Braithwaite, 2008). Increasing altitude provides favourable climatic conditions, i.e. decreasing temperatures and increasing precipitation directly leading to the formation of glaciers (Křížek & Mida, 2013). It has been found that glaciers situated at higher altitudes show less susceptibility towards depletion, i.e. their rate of retreat is lower, while glaciers at lower altitudes are retreating at faster rates. A study based on the Chandra basin in Himalayan glaciers has found that out of 18% of water loss of the total basin from the year 1984–2012, about 67% of the loss was reported from smaller and lower altitude glaciers (Tawde et al., 2017). The data for the altitude of the Gangotri basin has been obtained from the DEM (digital elevation model) and ASTER (Advanced Spaceborne Thermal Emission and Reflection Radiometer) project by USA and Japan in 2009. A digital elevation model (DEM) is a digital raster representation of ground surface topography or terrain. Each raster cell (or pixel) has a value corresponding to its altitude above sea level. ASTER's GDEM was created by stereo correlation of more than 1.2 million individual ASTER stereo scenes contained in the archive. The GDEM had 1 arc-second latitude and longitude postings (~30 m) and a vertical accuracy of approximately 10 m (Abrams et al., 2020).

Except obtaining, altitude raster, DEM dataset is used in terrain analysis and for extracting other terrain parameters such as slope and aspect, and modelling water flow and catchment modelling.

Slope

The *slope* or *gradient* of a [line](#) is a number that describes both the *direction* and the *steepness* of the line. The direction of a slope is significant as it offers information about the duration of incoming solar radiation. In the northern hemisphere, south-facing slopes receive solar radiation for longer duration in comparison to north-facing slopes. Therefore, the south-facing slopes are more prone to melting due to longer exposure to solar radiation (Wegmann et al., 1998). The steepness of slope determines the movement of glaciers under gravity (Evans, 2018). Slope is an important factor controlling the speed of glacier movement, together with their temperature, and amount of meltwater at the base of the glacier. Snow cover is expected to be low on steeper slopes. Therefore, slope of a glacier is expected to be an important factor behind glacier retreat, as the rate of retreat is directly controlled

by the slope of the glacier (Falaschi et al., 2017). It has been estimated that in the glaciers of the same climatic zones, different rates of retreat/advancement of glaciers can be explained by the mean slope and size of the glacier. In this study, slope in the glacier catchment area has been extracted from the ASTER DEM using GIS tools and techniques.

Insolation

Insolation, short for *incoming solar radiation*, is the incident energy of the Sun on any celestial body in a unit of area for a given time. One unit is Watt-hour/meter-square (WH/m²). In the context of Earth, not all the Sun's energy that strikes the earth actually reaches the surface. 30% of it gets reflected back by the atmosphere into space. Insolation is responsible for maintaining the temperature, and more insolation means higher temperature (Lund, 1968). Therefore, insolation is another factor affecting glacier cover. However, insolation is controlled by the topography of the surface and the interaction between slope, aspect and solar geometry, which decide the angle of incoming solar radiation. Insolation is also affected by any nearby higher landscape, which is responsible for shading the glaciers. The diffused radiation received from the sky is also affected by the nearby landscape, as it controls the proportion of the sky visible from the glacier (Bertoldi et al., 2010). Since Himalayan terrain is very undulating and has steep slopes (Kumar et al., 2021), the incoming solar radiation is greatly affected by the location of glaciers with respect to slope and aspect. The incoming solar radiation in this study has been calculated in a GIS environment. The tool calculates incoming solar radiation by using methods from the hemispherical view shed algorithm developed by Hetrick et al., 1993; Rich et al., 1995; Fu & Rich, 1999, 2002). The first step of calculation of incoming solar radiation involves the calculation of global radiation, i.e. total radiation of a particular area. Furthermore, the calculation of direct solar radiation is repeated for every feature or location of the topographic surface to generate an insolation map of the region.

$$\text{Global}_{\text{tot}} = \text{Dir}_{\text{tot}} + \text{Dif}_{\text{tot}} \quad (14.1)$$

where

Global_{tot} = total global radiation

Dir_{tot} = total direct radiation of all sun map sectors

Dif_{tot} = diffuse radiation of all sky map sectors

Total direct insolation (Dir_{tot}) for a given point is the sum total of the direct insolation (Dir_{0,α}) from all sun map sectors, which is calculated using the following equation:

$$\text{Dir}_{\text{tot}} = \Sigma \text{Dir}_{\theta,\alpha} \quad (14.2)$$

The direct insolation from the sun map sector, i.e. ($\text{Dir}_{\theta,\alpha}$) with a zenith angle of θ and azimuth angle of α is calculated using the following equation:

$$\text{Dir}_{\theta,\alpha} = S_{\text{Const}} * \beta^{m(\theta)} * \text{SunDur}_{\theta,\alpha} * \text{SunGap}_{\theta,\alpha} * \cos(\text{AngIn}_{\theta,\alpha}) \quad (14.3)$$

where

$S_{\text{Const}} = 1367 \text{ W/m}^2$

β = atmospheric transmissivity

$m(\theta)$ = relative optical path length

$\text{SunDur}_{\theta,\alpha}$ = time duration represented by the sky sector

$\text{SunGap}_{\theta,\alpha}$ = gap fraction for the sun map sector

$\text{AngIn}_{\theta,\alpha}$ = angle of incidence between the centroid of the sky sector and the normal

Land Surface Temperature

Temperature is the most important element of climate. Land surface temperature (LST) is a robust remote sensing-based method for the estimation of the temperature of the land surface. The impact of LST over glaciers is a well-recognized fact. Surface temperature is one of the most important parameters for estimating the effect of climatic change on glaciers. LST has a vast application in the study of glaciers. Brabyn & Stichbury, 2020, used LST to estimate the rate of thaw of ice sheet, while Mortimer et al., 2016, used MODIS LST data set to literally procure the temperature of the glacier surface. Wu et al., 2015, and Baral et al., 2020, also adopted LST to obtain glacier surface temperature. In this study, an attempt has been made to estimate surface temperatures from Landsat 5 ETM and Landsat 8 TIRS for Gangotri Glacier. Mono window algorithm using band 6 has been used for ETM, while the split window algorithm using bands 10 and 11 has been adopted for TIRS data. Mono Window algorithm has been used for LST calculation. The processes involved in the retrieval of LST are as follows:

Calculation of TOA (Top of Atmospheric) spectral radiance.

$$\text{TOA}(L) = M_L * (Q_{\text{cal}} + A_L) \quad (14.4)$$

where

M_L = band-specific multiplicative rescaling factor from the metadata of downloaded imagery (RADIANCE_MULT_BAND_x, where x is the band number)

Q_{cal} = corresponds to band 10

A_L = band-specific additive rescaling factor from the metadata of downloaded imagery (RADIANCE_ADD_BAND_x, where x is the band number)

TOA to Brightness Temperature conversion utilized the following formula:

$$BT = (K_2 / (\ln(K_1/L) + 1)) - 273.15 \quad (14.5)$$

where

K_1 = band-specific thermal conversion constant from the metadata of downloaded imagery ($K1_CONSTANT_BAND_x$, where x is the thermal band number).

K_2 = band-specific thermal conversion constant from the metadata of downloaded imagery ($K2_CONSTANT_BAND_x$, where x is the thermal band number).

Calculation of NDVI utilized the following formula:

$$NDVI = (NIR - RED) / (NIR + RED) \quad (14.6)$$

The formula for Landsat 5:

$$NDVI = (Band\ 4 - Band\ 3) / (Band\ 4 + Band\ 3) \quad (14.7)$$

where Band 4 is a near-infrared band and Band 3 is a visible red band in Landsat 5.

The formula for Landsat 8:

$$NDVI = (Band\ 5 - Band\ 4) / (Band\ 5 + Band\ 4) \quad (14.8)$$

where Band 5 is a near-infrared band and Band 4 is a visible red band in Landsat 8.

Calculation of the NDVI is important because, subsequently, the proportion of vegetation (P_v), which is highly related to the NDVI, and emissivity (ϵ), which is related to the P_v , must be calculated.

Calculation of the proportion of vegetation P_v utilized the following formula:

$$P_v = \text{Square}((NDVI - NDVI_{\min}) / (NDVI_{\max} - NDVI_{\min})) \quad (14.9)$$

Calculation of emissivity ϵ :

$$\epsilon = 0.004 * P_v + 0.986 \quad (14.10)$$

It is essential to calculate the land surface emissivity LSE(ϵ) in order to estimate LST, since the LSE is a proportionality factor that scales blackbody radiance (Planck's law) to predict emitted radiance, and it is the efficiency of transmitting thermal energy across the surface into the atmosphere (Jiménez-Muñoz & Sobrino, 2006). The land surface emissivity LSE (ϵ) is calculated as proposed by Sobrino and Jiménez-Muñoz et al., 2014.

Calculation of LST:

$$LST = BT / (1 + \lambda * (BT / \rho) * \ln(e))$$

where

BT = brightness (at satellite temperature)

λ = Wavelength of emitted radiance (0.00115)

ρ = 14,380 (Constant)

e = Emissivity

In order to deal with seasonal variation in temperature, taking mean annual temperature is a safe method. Therefore, in this study, LST is calculated on a quarterly basis. The member LST rasters for each reference year, thus, represent the mean LST value of all four seasons, i.e. summer, spring, autumn and winter.

Normalized Difference Snow Index

Normalized Difference Snow Index (NDSI) developed by Hall et al., 1995, is a remote-sensing method to map snow-cover area. It is a widely accepted method to study glacier dynamics and glacier expanse (Khan, 2019; Kulkarni et al., 2002; Yao et al., 2010). Here, one should acknowledge the optical properties and thermodynamics of ice and snow, having an albedo of 0.5–0.7, respectively, meaning that these surfaces reflect 50–70% of insolation (NSIDC, n.d.). Higher intrinsic albedo of snow and ice results in more radiative heat loss (Demenocal & Rind, 1993). While studying glaciers, Rose et al., 2017, explained the albedo-feedback of the snow, which accounted responsible for affecting the zonal energy budget. More snow-covered glacier catchment means a greater amount of radiative heat loss. Therefore, it is justified to assess the snow cover by the means of the NDSI method for an integrated catchment-level study of Gangotri. NDSI is a measure of the relative magnitude of the reflectance difference between visible (green) and shortwave infrared (SWIR). It controls the variance of two bands (one in the short-wave infrared and another one in the visible parts of the spectrum), which is suitable for snow mapping. The snow absorbs most of the shortwave radiance from the sun, but the cloud does not. Thus, the NDSI can effectively differentiate snow and cloud and, therefore, can be used, subsidiarily, in glacier monitoring.

$$NDSI = (GREEN - SWIR) / (GREEN + SWIR) \quad (14.11)$$

Formula for Landsat 5:

$$NDSI = (Band2 - BAND5) / (BAND2 + BAND5) \quad (14.12)$$

where Band 2 is a visible green band and Band 5 is short wave infrared band in Landsat 5.

Formula for Landsat 8:

$$\text{NDSI} = (\text{Band3} - \text{BAND6}) / (\text{BAND3} + \text{BAND6}) \quad (14.13)$$

where Band 3 is a visible green band and Band 6 is short-wave infrared band in Landsat 8.

In order to capture the correct amount of snow in the catchment, a quarterly mean NDIS is calculated for each reference year. The member NDSI raster, thus, represents the mean NDSI value of all four seasons, i.e. summer, spring, autumn and winter.

Methods

Principle Component Analysis

Principle component analysis (PCA) is a mathematical tool based on linear algebra that is used to reduce the dimensionality of a dataset. The dimensionality reduction is done by reduction of directions, i.e. principal component (PC) (Ringnér, 2008). In PCA, each PC is identified as a linear combination of variables, whereas the first principal component presents maximum variation (Wold et al., 1987). PCA can effectively be employed to procure the variables to analyse a phenomenon at an optimal level (Sarkar & Chouhan, 2021). In the process of data analysis, PCA is adopted to better discriminate the data (Adler & Golany, 2002) and to select the variables that are not equally important in explaining the given phenomena (Das et al., 2021). Lencioni et al., 2007, used PCA for ecological studies of glacier. Walsh & Butler, 1997, used PCA weights to monitor glacier debris flow for morphometric analysis using slope, aspect, sun angle and elevation.

Application of PCA: In this study, we require weights for the predictor variables for running fuzzy product algorithms over the rasters representing predictor variables. Eigenvalues of PCs are assigned as weights for predictor rasters in fuzzy product. For that purpose, it is most suitable to run PCA over all the pixels of predictor rasters to obtain eigenvalues that represent the whole raster rather than a sample of its pixels. To calculate eigenvalues of the predictor rasters i.e., elevation, slope, Insolation, LST and NDSI, a suitable GIS environment is utilized.

Random Forest Regression (RFR)

Within the last few decades, various predictive techniques have been used in civil and environmental engineering applications (Gislason et al., 2006; Pal et al. 2013; Were et al. 2015). In this research, we refer to RFR, which is an extension of a technique developed by Breiman, 2001, called random forest (RF) that has

outstanding performance with regard to predicting error. Having tree-structured predictors, injected with randomness, makes it an exceptionally robust predictor. It is a supervised machine learning method that uses ensemble learning (Bakshi, 2020) for regression by boosting and bagging and generates significantly unbiased estimations of generalized errors (Chakure, 2019). The decision trees randomly create training data and test data. The test data used to test the fitting of the model and the error is usually called 'out of bag error' or OOB. OOB error is expressed as:

$$\text{MSE}_{\text{OOB}} = n^{-1} \sum_1^n (y_i - \hat{y}_{\text{OOB}i})^2 \quad (14.14)$$

where $\hat{y}_{\text{OOB}i}$ is the mean of OOB predictions for i th observation.

Mean square residual (MSE) is another method of cross-validation. The lower the value, the better the fit of data. However, a value below 0.05 is safe for the validity of the results. MSR is mathematically expressed as:

$$y - \hat{y} = \hat{\epsilon},^2 \quad (14.15)$$

where y is observed value and \hat{y} and percent of variance explained are computed as:

$$1 - \frac{\text{MSE}_{\text{OOB}}^2}{\sigma_y^2} \quad (14.16)$$

where σ_y^2 is computed as a divisor with n (not as $n-1$).

RFR has been very popular in various scientific investigations of numerical relationships. It has been applied to remotely sensed data as well (Zhou et al., 2016), while Wangchuk & Bolch, 2020, applied this method to sentinel datasets for glacial mapping. RFR method has also been used in automatic glacier rock detection by Brenning, 2009. RF is a binary stepwise regressor that can explain mutual non-linear relationship (Brenning, 2009).

Application of RFR: In this study, the rationale to utilize RFR is to delve into the complexity of various factors that affect glacial dynamics. For modelling the potential zones of accumulation, equilibrium or ablation, it is of utmost importance that that we perform RFR that give Gini-impurity for all predictor variables and regress the values with explained variation. Thus, RFR is applied to predictor variables, i.e. elevation, slope, Insolation, LST and NDSI for validating their adoption for modelling the zones of glacial catchment. Pixel values of 251 random pixels (less than 10% of population according to central limit theorem) of the predictor variables are extracted using random sampling without replacement for the ML. RFR is performed using R version 3.6. cforest package is utilized for performing RFR in RStudio. Before running the algorithm, multicollinearity is visually checked for the reference years for all the variables. To train the data, 70% of the sample are selected, and n tree is tuned to 170. n tree 170 gives minimal test error (Figs. 14.5 and 14.6) and optimizes the accuracy for present modelling. For validation of results of RF MSE is used.

Fuzzy Overlay

Fuzzy overlay is based on Zadeh’s (1972) fuzzy theory (Hsieh & Chen, 1999) that allows the analysis of a phenomenon belonging to multiple sets. It explains the relationship between multiple members of the set. Unlike Boolean, it transforms the data onto a scale of 0 to 1 using the theory of partial truth (Kaur & Mahajan, 2015). 0 is given to the data points that are absolute non-members and 1 is given to the data points that are absolute members; however, there are various methods to perform the computation, ranging from fuzzy Sum, fuzzy And, fuzzy Or, fuzzy Gaussian and fuzzy product.

Application of Fuzzy Product: We, in this study, have utilized fuzzy products that multiply each of the values for all member rasters (DEM, slope, insolation, LST, NDSI) for each cell in a GIS environment. The eigenvalues (Tables 14.2 and 14.3) calculated through PCA are supplied as weights for fuzzy products for each corresponding year. The returned raster is then classified into accumulation, equilibrium and ablation zones. The threshold for classification of the returned raster for the zone of accumulation is 0–0.2; for the zone of equilibrium, the range is 0.2–0.36, and for zone of ablation, it is 0.36–0.99.

In this study, the reference period denotes a 20-year difference. Therefore, we argue that it is a short period of time for orogenic elevation increase or associated slope change; however, small avalanches have not been taken into account. We also assume that the insolation has remained constant over the 20 years. Thus, rasters of DEM, slope and insolation are kept uniform for both years. In each operation, NDSI and LST rasters are supplied accordingly.

Table 14.2 Accumulative Eigen values, 1995

| 1995 – Percent and accumulative eigenvalues | | | | |
|---|---|-------------|-------------------------|------------------------------|
| PC Layer | | Eigen value | Percent of Eigen values | Accumulative of Eigen values |
| Insolation | 1 | 0.04047 | 49.5870 | 49.5870 |
| LST | 2 | 0.02231 | 27.3319 | 76.9189 |
| Slope | 3 | 0.01151 | 14.1070 | 91.0260 |
| DEM | 4 | 0.00540 | 6.6178 | 97.6437 |
| NDSI | 5 | 0.00192 | 2.3563 | 100.0000 |

Table 14.3 Accumulative Eigen values, 2015

| 2015 – Percent and accumulative eigenvalues | | | | |
|---|---|-------------|-------------------------|------------------------------|
| PC Layer | | Eigen value | Percent of Eigen values | Accumulative of Eigen values |
| Insolation | 1 | 0.04143 | 48.3052 | 48.3052 |
| LST | 2 | 0.02315 | 26.9871 | 75.2923 |
| Slope | 3 | 0.01275 | 14.8612 | 90.1535 |
| DEM | 4 | 0.00476 | 5.5554 | 95.7089 |
| NDSI | 5 | 0.00368 | 4.2911 | 100.0000 |

Results

PCA

All causative factors are important in the modelling of the glacial zones of Gangotri, with varying degrees of importance. The potential zones of the ablation loosely coincide with LST variation across the catchment. However, the eigenvalues of PCA are highest for Insolation followed by LST, i.e. 50% and 27%, respectively. Slope and DEM account for only 14% and 7% of eigenvalues for the year 1995. For the year 2015, the order of variables remains constant, but percentage eigenvalue contribution changes where insolation contributes 48% followed by LST with 14%. Slope and DEM count 14% and 7% of eigenvalues, respectively. NDSI eigenvalues increased from 2% to 4% approximately from 1995 to 2015. All these values are case specific, and we propound no generalization.

Collinearity in Data

The visual assessment of the scatter plots for the reference years represents peculiar associations in the variables (Figs. 14.3 and 14.4). There is a strong negative correlation between NDSI and LST. The respective figures represent a strong positive correlation in slope and elevation of the catchment area. The scatter plot is also suggestive of a weak negative association between LST. The association of other variables is not explainable through the scatter plots.

RFR

The RFR for 1995 regresses the values of predictor variables at an MSE (Eq. 14.15) of 0.019 and the variance explained is 41.16%. The values of the mean of MSE remain 0.020 and the variance explained 41.4% for 2015. Error plots for RF through minimal error at 170 ntree for both reference years, i.e. 1995 and 2015 (Figs. 14.5 and 14.6).

Fuzzy Product

The member rasters (*map a*, *map b*, *map c*, *map d*, *map e*, *map f*, *map g*) are together (Fig. 14.7) supplied to the GIS environment for running fuzzy products with corresponding weights. The returned rasters produce interesting results. The result demonstrates a vast increase in the potential ablation zone of the glacial catchment

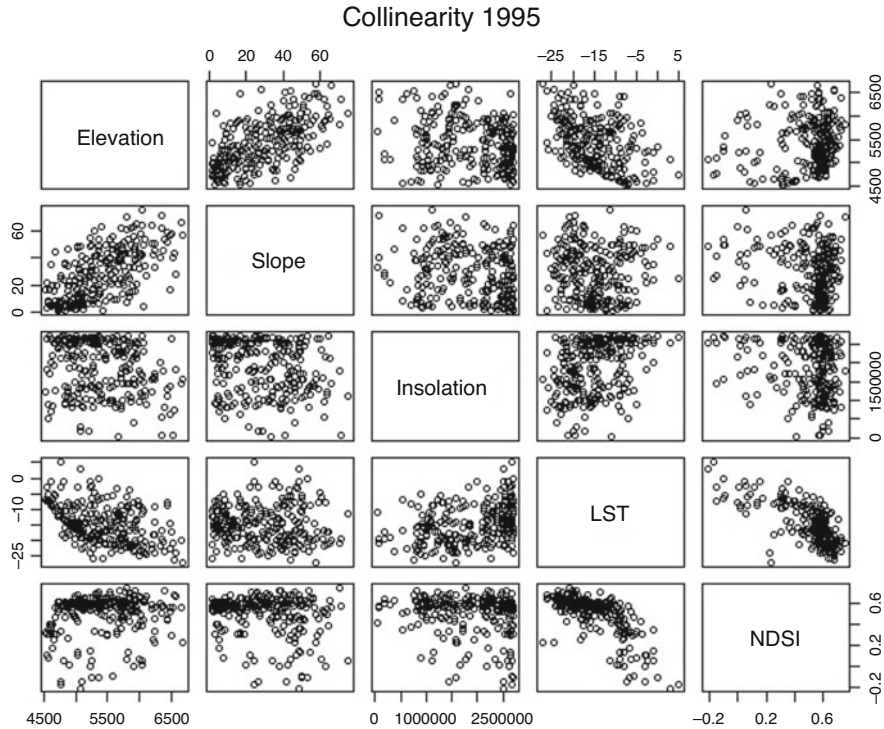


Fig. 14.3 Collinearity of data, 1995

over the period of 1995 and 2015 (map h and map j). The increase in the potential ablation zone is more prominent on the south-facing slope, whereas the potential equilibrium zone and potential accumulation zone seem to have depleted much more in lower elevation areas. The higher latitudes and north-facing slopes represent minimal changes.

The study propounds a vast increase in the areal extent of the potential ablation zone over the period of 1995 and 2015, expanding over threefold of what it used to be in 1995. The areal increase in the potential ablation zone has taken place at the expense of the potential accumulation zone and potential equilibrium zones (Fig. 14.8).

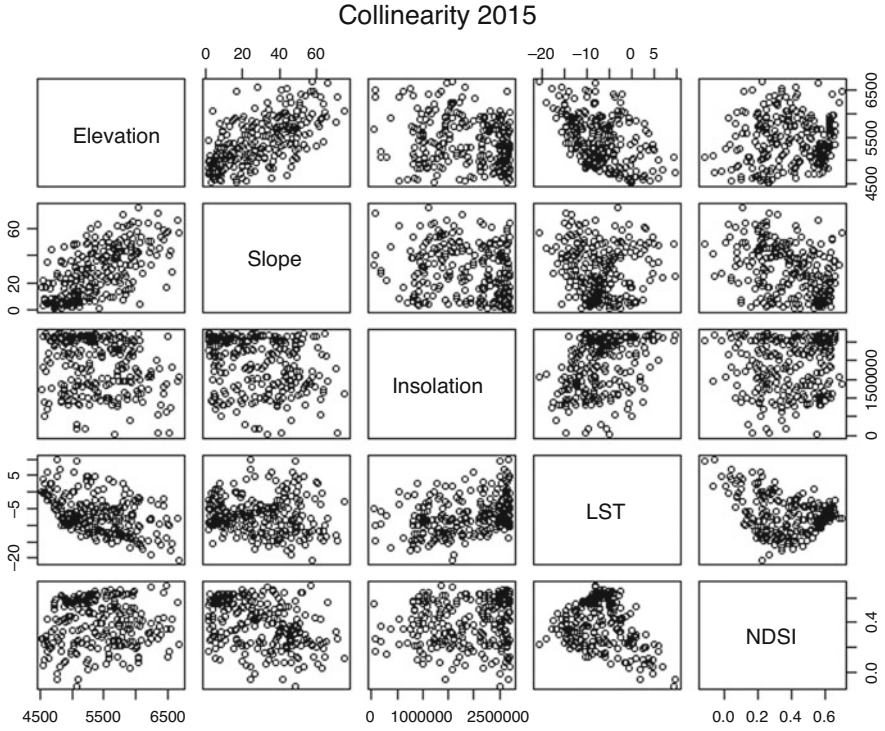


Fig. 14.4 Collinearity of data, 2015

Fig. 14.5 Error Plot, 1995

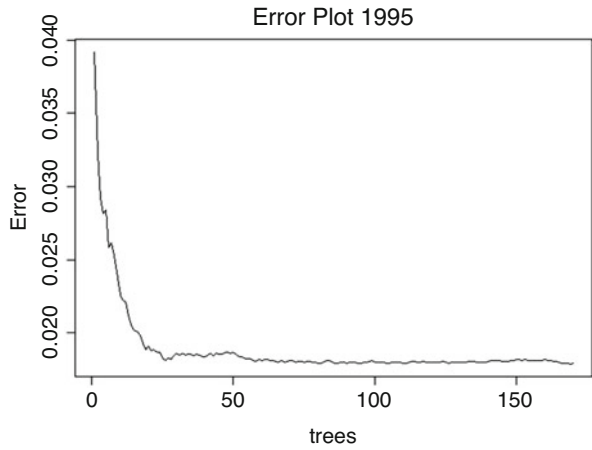


Fig. 14.6 Error Plot, 2015

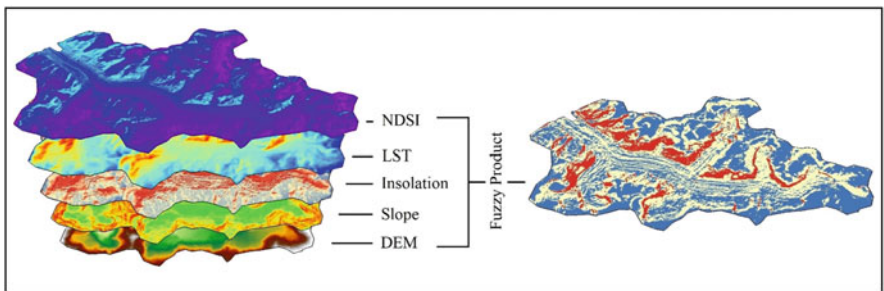
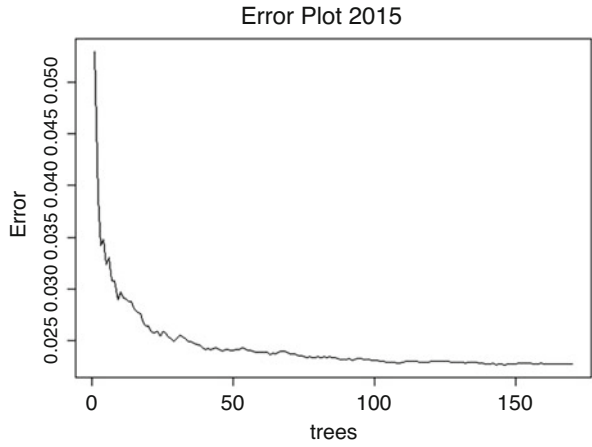


Fig. 14.7 Input raster and resultant raster

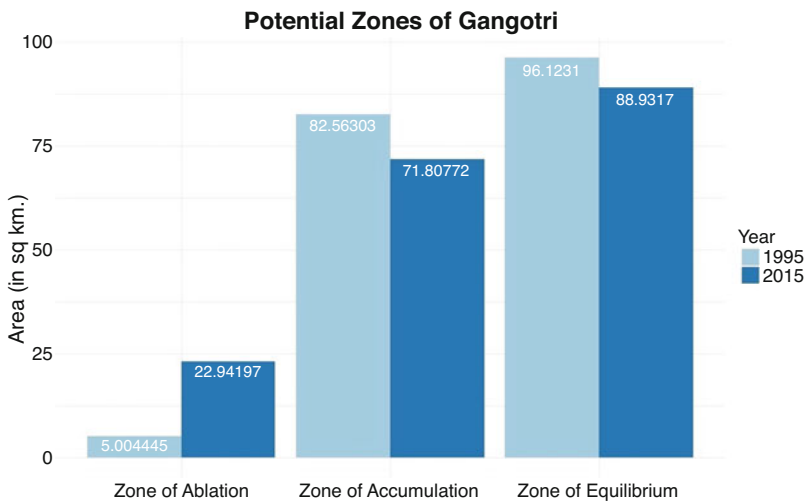
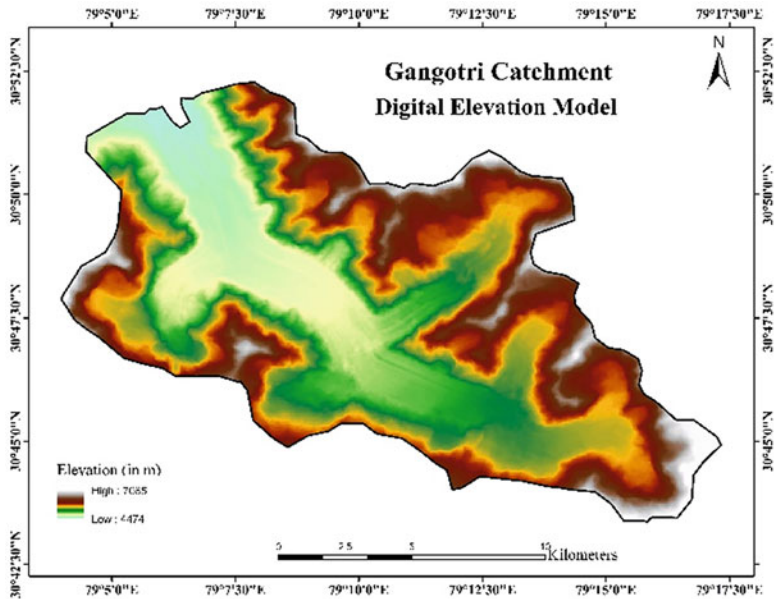
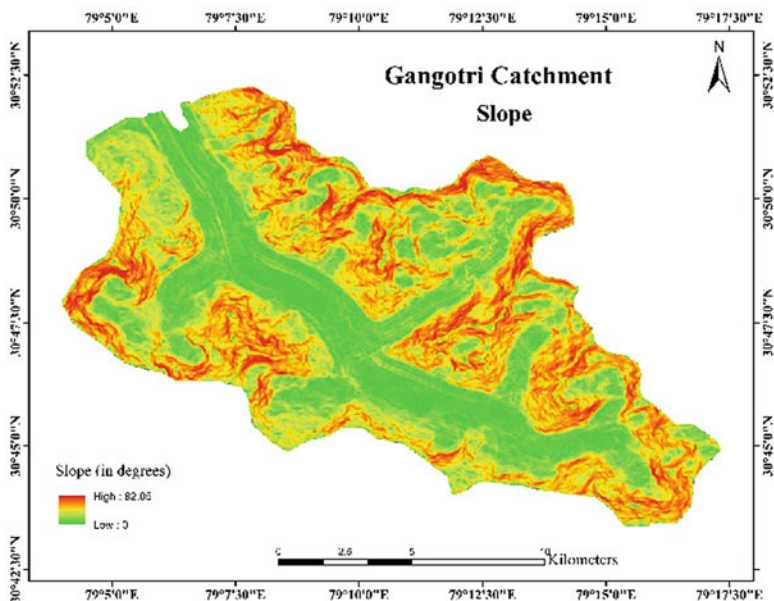


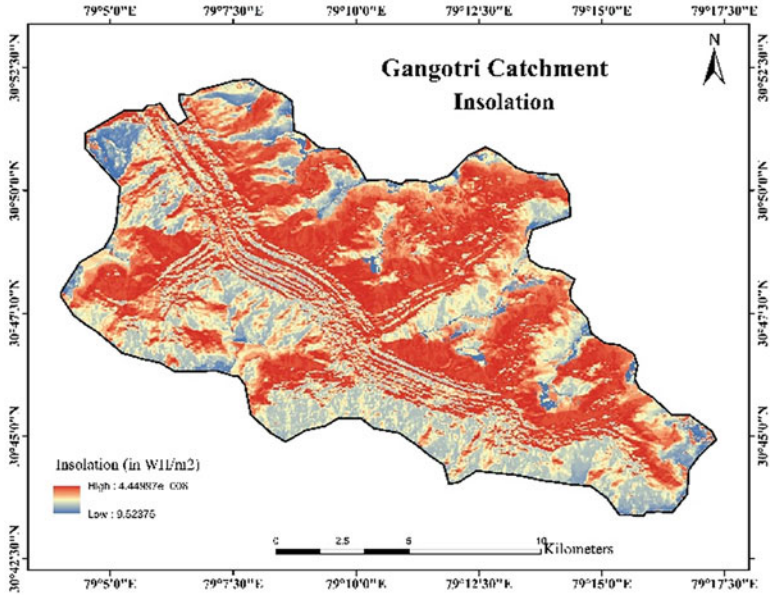
Fig. 14.8 Area under different potential zones of Gangotri



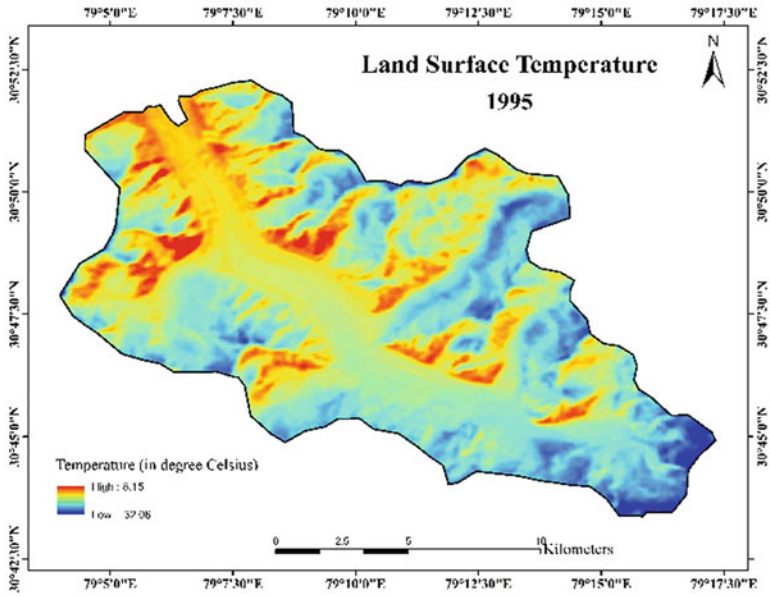
Map a: Digital elevation model



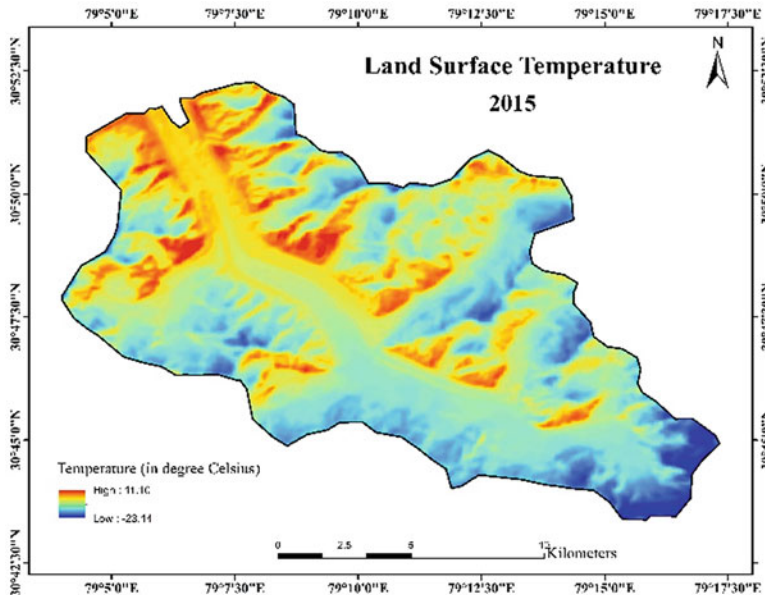
Map b: Slope



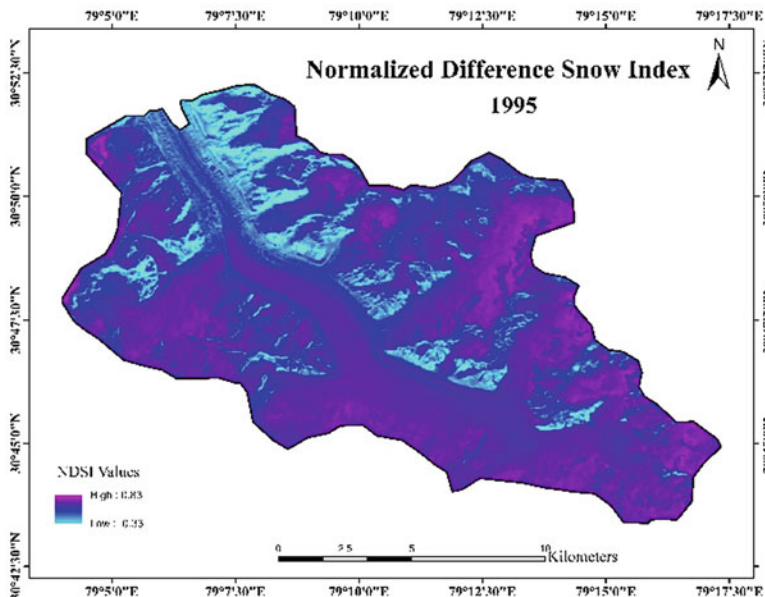
Map c: Insolation



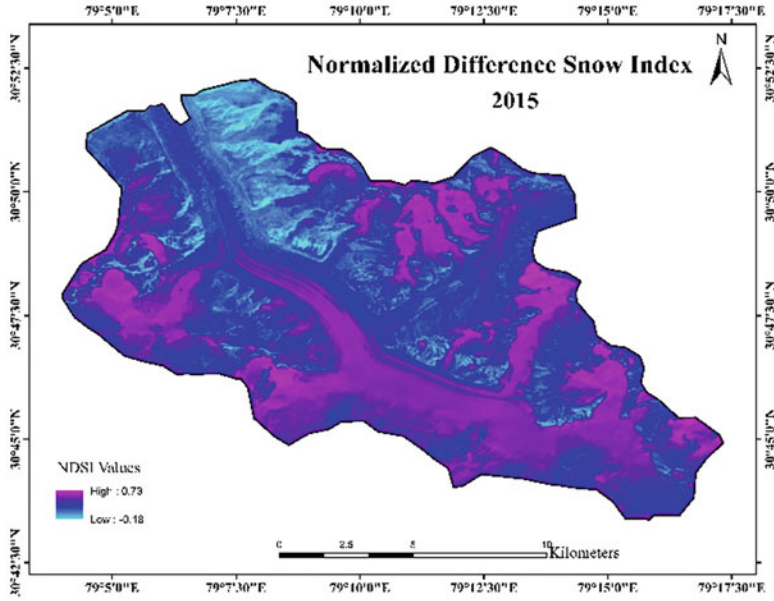
Map d: Land surface temperature, 1995



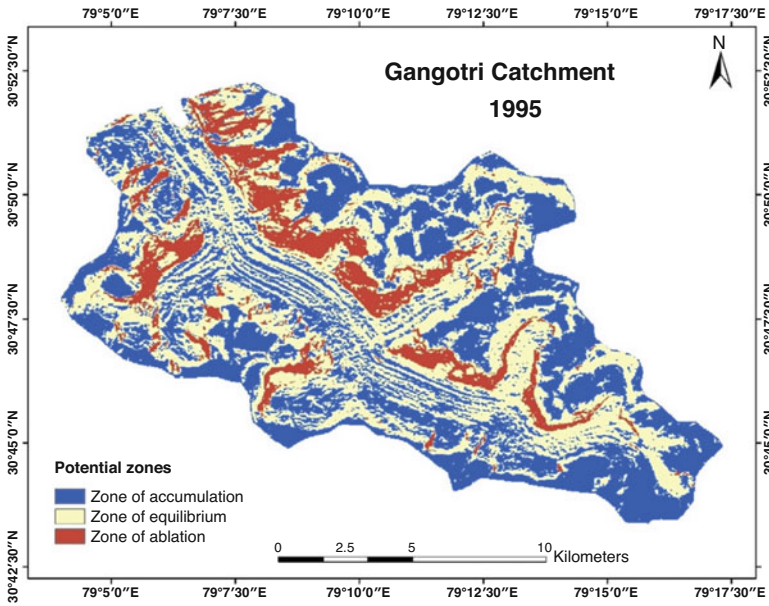
Map e: Land surface temperature, 2015



Map f: NDSI, 1995

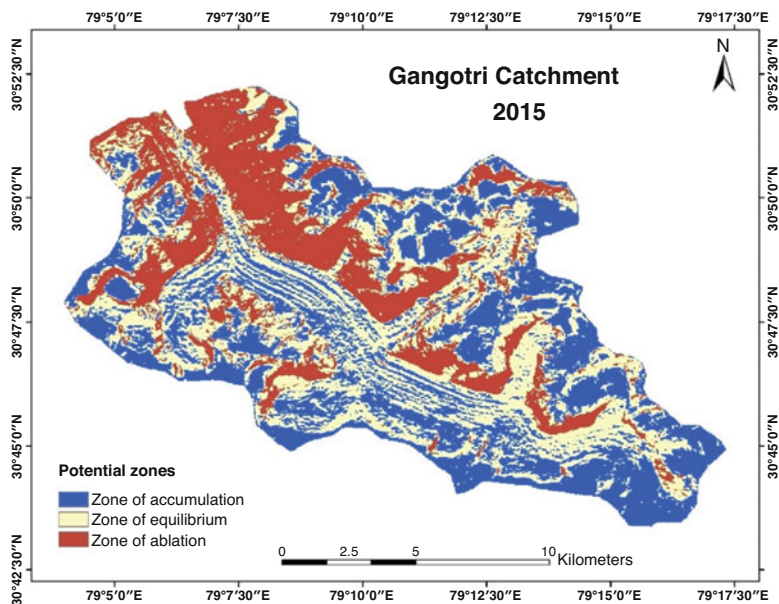


Map g: NDSI, 2015



map h: Potential zones of glacial dynamics, 1995

Map h: Potential zones of glacial dynamics, 1995



map i: Potential zones of glacial dynamics, 2015

Map i: Potential zones of glacial dynamics, 2015

Discussion and Conclusion

Gangotri glacier is receding in space over time, and a large glacial mass has been claimed by rising temperatures. The accumulation zone is retreating, and the ablation zone is increasing in the area (Haritashya et al., 2006). It appears that an increase in the ablation zone is very crucial for the sustenance of a glacier (Oerlemans, 1991) and a very strong negative sign for the health of the glacier (Agrawal et al., 2018). This study confirms the increase in the potential ablation zone of Gangotri from 1995 and 2015 at the expense of potential zones of equilibrium and accumulation. However, it is noteworthy that the zoning glacier is based on the potential outcomes of member rasters, which does not represent the true ablation, equilibrium or accumulation zone of Gangotri.

Fuzzy overlay operations have been used for demarcating hierarchical zones of complex geographical phenomena. Through GIS, input of causative rasters can be re-scaled and integrated generating a single raster that can be reclassified in multiple zones. Unlike weighted overlay, this method defines possibility rather than probability, and therefore, the membership of a causative raster is immune to assigned weights (Ahmed et al., 2014). Scholars have gone to great lengths to propound the significance of these methods for mapping suitable zones or susceptible zones for a specific phenomenon (Dimri et al., 2007; Kayastha et al., 2013; Kumar et al., 2013).

For instance, the fuzzy AHP method was used by Kumar et al., 2021, to demarcate potential zones of groundwater. The application of fuzzy overlay combined with dimensionality reduction methods is limited for glacial studies. Most of the previous GIS-based inventory research focuses on the glacial retreat in Gangotri (Singh et al., 2017; Ghosh 2017; Sparavigna, 2017) where due importance is not given to the zonal dynamics. The role of topographical causative factors is not modelled at large by scholars like Ding (2010), Rai et al. (2017). In this study, we combine the fuzzy product method with PCA to demarcate the potential zones of glacial mass balance along with the statistically significant result of RFR. We have to acknowledge that the modelled potential zones of glaciers are estimations and have limited capacity to represent the true processes and mass balance of the glaciers.

The objective of this chapter is to model and analyse the dynamics of Gangotri in the wake of underlying physiological factors in association with climatic factor, i.e. temperature. The study is one of its kind where for the first time role topography is modelled for glacial zonation of Gangotri catchment using the fuzzy product overly method, and the mutual relationship of various predictive variables is assessed with ML. Glacial zones are essential sub-units of a glacier, and each one is important to understand the glacial mass balance. This study puts forth the spatial extent of these zones for Gangotri and compares it with two time periods and, thus, highlights the gravity of climate change by areal quantification of the potential for glacial mass loss.

This study concludes that the Gangotri glacier is experiencing climate-imposed vulnerability and is prone to further loss of ice mass. The areal increase in the potential zone of ablation in the catchment poses higher risks of glacial losses against reduced possibility of replenishment from fresh snow at the catchment level. Being an alpine glacier, the dynamics are complex in association with topographical heterogeneity. Glacial zones coincide with slope, and physiology seems to have a key role in glacial dynamics and zonation. Hence, the study strongly suggests the inclusion of physiological factors in holistic glacial studies. Gangotri crucially contributes to India's fluvial system and, therefore, its thorough analyses are of key importance, and quantification of risks and vulnerabilities of the glacier both in situ and ex situ causative factors are worth delving.

Fuzzy product combined with PCA eigenvalues produces reasonable results for the potential glacier zone modelling and, hence, can be safely used for glacial studies in the future. Regression methods are useful to explain the mutual relationship of the various predictive variables. This study is a stand-alone piece of research that opens up a new arena for alpine glacial studies.

References

- Abrams, M., Crippen, R., & Fujisada, H. (2020). ASTER global digital elevation model (GDEM) and ASTER global water body dataset (ASTWBD). *Remote Sensing*, 12(7), 1156.

- Adler, N., & Golany, B. (2002). Including principal component weights to improve discrimination in data envelopment analysis. *Journal of the Operational Research Society*, 53(9), 985–991.
- Agrawal, A., Thayyen, R. J., & Dimri, A. P. (2018). Mass-balance modelling of Gangotri glacier. *Geological Society, London, Special Publications*, 462(1), 99–117.
- Ahmed, M. F., Rogers, J. D., & Ismail, E. H. (2014). A regional level preliminary landslide susceptibility study of the upper Indus river basin. *European Journal of Remote Sensing*, 47(1), 343–373.
- Aigang, L., Tianming, W., Shichang, K., & Deqian, P. (2009). On the relationship between latitude and altitude temperature effects. In *2009 International Conference on Environmental Science and Information Application Technology* (Vol. 2, pp. 55–58). IEEE.
- Ambinakudige, S. (2010). A study of the Gangotri glacier retreat in the Himalayas using Landsat satellite images. *International Journal of Geoinformatics*, 6(3), 7.
- Arndt, E., & Schembri, P. J. (2015). Common traits associated with establishment and spread of Lessepsian fishes in the Mediterranean Sea. *Marine Biology*, 162, 2141–2153.
- Arora, M., & Malhotra, J. (2023). Prevalent climate variables during ablation season around Gangotri glacier. In *Climate change and environmental impacts: Past, present and future perspective* (pp. 205–214). Springer International Publishing.
- Bahuguna, I. M. (2003). Satellite stereo data analysis in snow and glaciated region. In *Training document: Course on remote sensing for glaciological studies; Manali, India* (pp. 85–99). SAC/RESA/MWRG/ESHD/TR.
- Bakshi, C. (2020). *Random forest regression*. Retrieved 23 February 2022, from <https://levelup.gitconnected.com/random-forest-regression-209c0f354c84>
- Banerjee, A., & Shankar, R. (2013). On the response of Himalayan glaciers to climate change. *Journal of Glaciology*, 59(215), 480–490.
- Baral, P., Haq, M. A., & Yaragal, S. (2020). Assessment of rock glaciers and permafrost distribution in Uttarakhand, India. *Permafrost and Periglacial Processes*, 31(1), 31–56.
- Bertoldi, G., Notarnicola, C., Leitinger, G., Endrizzi, S., Zebisch, M., Della Chiesa, S., & Tappeiner, U. (2010). Topographical and ecohydrological controls on land surface temperature in an alpine catchment. *Ecohydrology: Ecosystems, Land and Water Process Interactions, Ecohydrogeomorphology*, 3(2), 189–204.
- Bhambri, R., Bolch, T., & Chaujar, R. K. (2012). Frontal recession of Gangotri glacier, Garhwal Himalayas, from 1965 to 2006, measured through high-resolution remote sensing data. *Current Science*, 102(3), 489–494.
- Bisht, K., Joshi, Y., Upadhyay, S., & Metha, P. (2018). Recession of Milam glacier, Kumaun Himalaya, observed via lichenometric dating of moraines. *Journal of the Geological Society of India*, 92(2), 173–176.
- Bolch, T., Kulkarni, A., Kääb, A., Huggel, C., Paul, F., Cogley, J. G., et al. (2012). The state and fate of Himalayan glaciers. *Science*, 336(6079), 310–314.
- Brabyn, L., & Stichbury, G. (2020). Calculating the surface melt rate of Antarctic glaciers using satellite-derived temperatures and stream flows. *Environmental Monitoring and Assessment*, 192(7), 1–14.
- Braithwaite, R. J. (2008). Temperature and precipitation climate at the equilibrium-line altitude of glaciers expressed by the degree-day factor for melting snow. *Journal of Glaciology*, 54(186), 437–444.
- Breiman, L. (2001). Random forests. *Machine Learning*, 45, 5–32.
- Brenning, A. (2009). Benchmarking classifiers to optimally integrate terrain analysis and multi-spectral remote sensing in automatic rock glacier detection. *Remote Sensing of Environment*, 113(1), 239–247.
- Chakure, A. (2019). *Random forest and its implementation*. Retrieved 23 February 2022, from <https://medium.com/swlh/random-forest-and-its-implementation-71824ced454f>
- Chaujar, R. K. (2009). Climate change and its impact on the Himalayan glaciers—a case study on the Chorabari glacier, Garhwal Himalaya, India. *Current Science*, 703–708.

- Clark, P. U., Pisias, N. G., Stocker, T. F., & Weaver, A. J. (2002). The role of the thermohaline circulation in abrupt climate change. *Nature*, *415*(6874), 863–869.
- Das, M., Das, A., Giri, B., Sarkar, R., & Saha, S. (2021). Habitat vulnerability in slum areas of India—What we learnt from COVID-19? *International Journal of Disaster Risk Reduction*, *65*, 102553.
- Demenocal, P. B., & Rind, D. (1993). Sensitivity of Asian and African climate to variations in seasonal insolation, glacial ice cover, sea surface temperature, and Asian orography. *Journal of Geophysical Research: Atmospheres*, *98*(D4), 7265–7287.
- Dimri, S., Lakhera, R. C., & Sati, S. (2007). Fuzzy-based method for landslide hazard assessment in active seismic zone of Himalaya. *Landslides*, *4*(2), 101–111.
- Ding, J. (2010). Retreating glaciers of the Himalayas: A case study of gangotri glacier using 1990–2009 satellite images.
- Evans, D. J. (2018). *Glaciation: A very short introduction*. Oxford University Press.
- Falaschi, D., Bolch, T., Rastner, P., Lenzano, M. G., Lenzano, L., & VECCHIO, A. L., & Moragues, S. (2017). Mass changes of alpine glaciers at the eastern margin of the northern and southern Patagonian Icefields between 2000 and 2012. *Journal of Glaciology*, *63*(238), 258–272.
- Forsberg, R., Sørensen, L., & Simonsen, S. (2017). Greenland and Antarctica ice sheet mass changes and effects on global sea level. *Integrative Study of the Mean Sea Level and Its Components*, 91–106.
- Fu, P., & Rich, P. M. (1999). Design and implementation of the solar analyst: An ArcView extension for modeling solar radiation at landscape scales. In *proceedings of the nineteenth annual ESRI user conference* (Vol. 1, pp. 1–31). USA: San Diego.
- Fu, P., & Rich, P. M. (2002). A geometric solar radiation model with applications in agriculture and forestry. *Computers and Electronics in Agriculture*, *37*(1–3), 25–35.
- Gasson, E., DeConto, R., & Pollard, D. (2015). Antarctic bedrock topography uncertainty and ice sheet stability. *Geophysical Research Letters*, *42*(13), 5372–5377.
- Ghosh, P. (2017). Remote sensing and GIS analysis of Gaumukh snout retreat and ice loss estimation at Gangotri glacier, during 1962–2015. *Global Journal of Current Research*, *5*(3), 113–119.
- Gislason, P. O., Benediktsson, J. A., & Sveinsson, J. R. (2006). Random forests for land cover classification. *Pattern Recognition Letters*, *27*(4), 294–300.
- Hall, D. K., Riggs, G. A., & Salomonson, V. V. (1995). Development of methods for mapping global snow cover using moderate resolution imaging spectroradiometer data. *Remote Sensing of Environment*, *54*(2), 127–140.
- Haritashya, U. K., Singh, P., Kumar, N., & Gupta, R. P. (2006). Suspended sediment from the Gangotri glacier: Quantification, variability and associations with discharge and air temperature. *Journal of Hydrology*, *321*(1–4), 116–130.
- Hetrick, W. A., Rich, P. M., Barnes, F. J., & Weiss, S. B. (1993). GIS-based solar radiation flux models. In *ACSM ASPRS annual convention* (Vol. 3, pp. 132–132). American Soc Photogrammetry & Remote Sensing+ Amer Cong On.
- Hsieh, C. H., & Chen, S. H. (1999). A model and algorithm of fuzzy product positioning. *Information Sciences*, *121*(1–2), 61–82.
- Jarvis, W. T. (2012). Integrating groundwater boundary matters into catchment management. In *The dilemma of boundaries* (pp. 161–176). Springer.
- Jiménez-Muñoz, J. C., & Sobrino, J. A. (2006). Error sources on the land surface temperature retrieved from thermal infrared single channel remote sensing data. *International Journal of Remote Sensing*, *27*(5), 999–1014.
- Jones, D. B., Harrison, S., Anderson, K., Selley, H. L., Wood, J. L., & Betts, R. A. (2018). The distribution and hydrological significance of rock glaciers in the Nepalese Himalaya. *Global and planetary change*, *160*, 123–142.
- T. D. (2015). Climate change rule of thumb: Cold “things” warming faster than warm things | NOAA [Climate.gov](https://www.noaa.gov). Retrieved 31 January 2022, from [https://](https://www.noaa.gov)

www.climate.gov/news-features/blogs/beyond-data/climate-change-rule-thumb-cold-things-warming-faster-warm-things

- Joshi, S., Khobragade, S., & Kumar, S. (2020). Spatio-temporal variability in glacier melt contribution in Bhagirathi river discharge in the headwater region of Himalaya.
- Kargel, J. S., Cogley, J. G., Leonard, G. J., Haritashya, U., & Byers, A. (2011). Himalayan glaciers: The big picture is a montage. *Proceedings of the National Academy of Sciences*, 108(36), 14709–14710.
- Kaur, J., & Mahajan, M. (2015). Hybrid of fuzzy logic and random Walker method for medical image segmentation. *IJ Image, Graphics and Signal Processing*, 7(2), 23.
- Kayastha, P., Bijuochhen, S. M., Dhital, M. R., & De Smedt, F. (2013). GIS based landslide susceptibility mapping using a fuzzy logic approach: A case study from Ghurmi-Dhad Khola area, eastern Nepal. *Journal of the Geological Society of India*, 82(3), 249–261.
- Khan, Z. (2019). *Tracing dynamics of snow cover in Pithoragarh district using geo-spatial techniques*. Aligarh Muslim University Aligarh, India.
- Kong, Y., Wang, K., Pu, T., & Shi, X. (2019). Nonmonsoon precipitation dominates groundwater recharge beneath a monsoon-affected glacier in Tibetan plateau. *Journal of Geophysical Research: Atmospheres*, 124(20), 10913–10930.
- Křížek, M., & Mida, P. (2013). The influence of aspect and altitude on the size, shape and spatial distribution of glacial cirques in the high Tatras (Slovakia, Poland). *Geomorphology*, 198, 57–68.
- Kulkarni, A. V., Srinivasulu, J., Manjul, S. S., & Mathur, P. (2002). Field based spectral reflectance studies to develop NDSI method for snow cover monitoring. *Journal of the Indian Society of Remote Sensing*, 30(1), 73–80.
- Kumar, U., Kumar, B., & Mallick, N. (2013). Groundwater prospects zonation based on RS and GIS using fuzzy algebra in Khoh River watershed, Pauri-Garhwal District, Uttarakhand, India. *Global Perspectives on Geography (GPG)*, 1(3), 37–45.
- Kumar, D., Singh, A., & Israil, M. (2021). Necessity of terrain correction in Magnetotelluric data recorded from Garhwal Himalayan region. *India. Geosciences*, 11(11), 482.
- Lencioni, V., Maiolini, B., Marziali, L., Lek, S., & Rossaro, B. (2007). Macroinvertebrate assemblages in glacial stream systems: A comparison of linear multivariate methods with artificial neural networks. *Ecological Modelling*, 203(1–2), 119–131.
- Liljedahl, A. K., Gädeke, A., O'Neel, S., Gatesman, T. A., & Douglas, T. A. (2017). Glacierized headwater streams as aquifer recharge corridors, subarctic Alaska. *Geophysical Research Letters*, 44(13), 6876–6885.
- Lund, I. A. (1968). Relationships between insolation and other surface weather observations at Blue Hill, Massachusetts. *Solar Energy*, 12(1), 95–106.
- Mitra, A., Banerjee, K., Sengupta, K., & Gangopadhyay, A. (2009). Pulse of climate change in Indian Suindarbans: A myth or reality? *National Academy Science Letters (India)*, 32(1), 19.
- Mortimer, C. A., Sharp, M., & Wouters, B. (2016). Glacier surface temperatures in the Canadian high Arctic, 2000–2015. *Journal of Glaciology*, 62(235), 963–975.
- Naithani, A. K., Nainwal, H. C., Sati, K. K., & Prasad, C. (2001). Geomorphological evidences of retreat of the Gangotri glacier and its characteristics. *Current Science*, 87–94.
- Oerlemans, J. (1991). The mass balance of the Greenland ice sheet: Sensitivity to climate change as revealed by energy-balance modelling. *The Holocene*, 1(1), 40–48.
- Pal, M., Singh, N. K., & Tiwari, N. K. (2013). Pier scour modelling using random forest regression. *ISH Journal of Hydraulic Engineering*, 19(2), 69–75.
- Paxman, G. J., Jamieson, S. S., Ferraccioli, F., Bentley, M. J., Forsberg, R., Ross, N., et al. (2017). Uplift and tilting of the Shackleton range in East Antarctica driven by glacial erosion and normal faulting. *Journal of Geophysical Research: Solid Earth*, 122(3), 2390–2408.
- Pörtner, H. O., Roberts, D. C., Adams, H., Adler, C., Aldunce, P., Ali, E., et al. (2022). *Climate change 2022: Impacts, adaptation and vulnerability* (p. 3056). IPCC.

- Ramsankaran, R. A. A. J., Navinkumar, P. J., Dashora, A., & Kulkarni, A. V. (2021). UAV-based survey of glaciers in Himalayas: Challenges and recommendations. *Journal of the Indian Society of Remote Sensing*, 49(5), 1171–1187.
- Rai, P. K., Mishra, V. N., Singh, S., Prasad, R., & Nathawat, M. S. (2017). Remote sensing-based study for evaluating the changes in glacial area: a case study from Himachal Pradesh, India. *Earth Systems and Environment*, 1, 1–13.
- Ray, K. (2009). *Snowline recedes on the Himalayas by 400 mts*. Retrieved 1 March 2022, from <https://www.deccanherald.com/content/23732/snowline-recedes-himalayas-400-mts.html>
- Rich, P. M., Hetrick, W. A., & Saving, S. C. (1995). *Modeling topographic influences on solar radiation: A manual for the SOLARFLUX model* (no. LA-12989-M). Los Alamos National Lab. (LANL), Los Alamos, NM (United States).
- Ringnér, M. (2008). What is principal component analysis? *Nature Biotechnology*, 26(3), 303–304.
- Rose, B. E., Cronin, T. W., & Bitz, C. M. (2017). Ice caps and ice belts: The effects of obliquity on ice – Albedo feedback. *The Astrophysical Journal*, 846(1), 28.
- Sarkar, A., & Chouhan, P. (2021). COVID-19: District level vulnerability assessment in India. *Clinical Epidemiology and Global Health*, 9, 204–215.
- Shi, S., Xu, H., Shui, Y., Liu, D., Xie, Q., Zhang, J., et al. (2023). Sedimentary organic molecular compositions reveal the influence of glacier retreat on ecology on the Tibetan plateau. *Science of the Total Environment*, 163629, 163629.
- Singh, D. S., Tangri, A. K., Kumar, D., Dubey, C. A., & Bali, R. (2017). Pattern of retreat and related morphological zones of Gangotri glacier, Garhwal Himalaya, India. *Quaternary International*, 444, 172–181.
- Singh, D. K., Thakur, P. K., Naithani, B. P., & Kaushik, S. (2018). Temporal monitoring of glacier change in Dhauliganga basin, Kumaun Himalaya using geo-spatial techniques. *ISPRS Annals of Photogrammetry, Remote Sensing & Spatial Information Sciences*, 4(5), 203.
- Sobrino, J. A., & Jiménez-Muñoz, J. C. (2014). Minimum configuration of thermal infrared bands for land surface temperature and emissivity estimation in the context of potential future missions. *Remote Sensing of Environment*, 148, 158–167.
- Sparavigna, A. C. (2017). The retreat of the terminus of Gangotri glacier in Google earth images.
- Tawde, S. A., Kulkarni, A. V., & Bala, G. (2017). An estimate of glacier mass balance for the Chandra basin, western Himalaya, for the period 1984–2012. *Annals of Glaciology*, 58(75pt2), 99–109.
- Thayyen, R. J., & Gergan, J. T. (2010). Role of glaciers in watershed hydrology: A preliminary study of a “Himalayan catchment”. *The Cryosphere*, 4(1), 115–128.
- Varugu, B. K., & Rao, Y. S. (2016, May). Glacier retreat monitoring from SAR coherence images: Application to Gangotri glacier. In *Land surface and cryosphere remote sensing III* (Vol. 9877, p. 987715). International Society for Optics and Photonics.
- Verma, A., Tiwari, S. K., Kumar, A., Sain, K., Rai, S. K., & Kumari, S. (2021). Assessment of water recharge source of geothermal systems in Garhwal Himalaya (India). *Arabian Journal of Geosciences*, 14(22), 1–18.
- Walsh, S. J., & Butler, D. R. (1997). Morphometric and multispectral image analysis of debris flows for natural hazard assessment. *Geocarto International*, 12(1), 59–70.
- Wangchuk, S., & Bolch, T. (2020). Mapping of glacial lakes using Sentinel-1 and Sentinel-2 data and a random forest classifier: Strengths and challenges. *Science of Remote Sensing*, 2, 100008.
- Wegmann, M., Gudmundsson, G. H., & Haeberli, W. (1998). Permafrost changes in rock walls and the retreat of alpine glaciers: A thermal modelling approach. *Permafrost and Periglacial Processes*, 9(1), 23–33.
- Were, K., Bui, D. T., Dick, Ø. B., & Singh, B. R. (2015). A comparative assessment of support vector regression, artificial neural networks, and random forests for predicting and mapping soil organic carbon stocks across an Afromontane landscape. *Ecological Indicators*, 52, 394–403.
- Wold, S., Geladi, P., Esbensen, K., & Öhman, J. (1987). Multi-way principal components-and PLS-analysis. *Journal of Chemometrics*, 1(1), 41–56.

- Wu, Y., Wang, N., He, J., & Jiang, X. (2015). Estimating mountain glacier surface temperatures from Landsat-ETM+ thermal infrared data: A case study of Qiyi glacier, China. *Remote Sensing of Environment*, 163, 286–295.
- Yao, X., Zhu, Y., Tian, Y., Feng, W., & Cao, W. (2010). Exploring hyperspectral bands and estimation indices for leaf nitrogen accumulation in wheat. *International Journal of Applied Earth Observation and Geoinformation*, 12(2), 89–100.
- Yu, W., Yao, T., Kang, S., Pu, J., Yang, W., Gao, T., et al. (2013). Different region climate regimes and topography affect the changes in area and mass balance of glaciers on the north and south slopes of the same glacierized massif (the west Nyainqentanglha range, Tibetan Plateau). *Journal of Hydrology*, 495, 64–73.
- Zadeh, L. A. (1972). A fuzzy-set-theoretic interpretation of linguistic hedges.
- Zhou, X., Zhu, X., Dong, Z., & Guo, W. (2016). Estimation of biomass in wheat using random forest regression algorithm and remote sensing data. *The Crop Journal*, 4(3), 212–219.